

OXIDO- AND DIOXIDOVANADIUM(V) COMPLEXES WITH O-VANILLIN SEMICARBAZONE: SYNTHESIS AND CRYSTAL STRUCTURE

Lidia Cuba^a, Paulina Bourosh^b, Victor Kravtsov^b, Elena Gorincioi^a, Diana Dragancea^{a*}

^aInstitute of Chemistry, 3, Academiei str., Chisinau MD-2028, Republic of Moldova

^bInstitute of Applied Physics, 5, Academiei str., Chisinau MD-2028, Republic of Moldova

*e-mail: ddragancea@gmail.com; phone: (+373 22) 739 790; fax: (+37 22) 739 954

Abstract. Two mononuclear oxido- and dioxidovanadium(V) coordination compounds [VO(HL)(EtO)(EtOH)_{0.6}(H₂O)_{0.4}][VO(HL)(SO₄)(EtO)]·0.4EtOH (**1**) and [VO₂(HL)]·2H₂O (**2**) have been prepared by reactions of *o*-vanillin semicarbazone (H₂L) with VOSO₄·5H₂O and NH₄VO₃ in 1:2 and 1:1 molar ratios in alcohol and alcohol/ammonia mixture. The single crystal X-ray diffraction study shows that in these compounds, the monoanionic HL⁻ organic ligand with deprotonated hydroxy group coordinates in the ONO tridentate mode, and the methoxy-group does not participate in coordination to the metal center. Compound **1** comprises complex cations and complex anions with VO³⁺ core and distorted octahedral geometries of vanadium atom. In complex **2**, vanadium has a distorted square-pyramidal environment typical for complexes with VO₂⁺ core.

Keywords: oxidovanadium(V), dioxidovanadium(V), *o*-vanillin semicarbazone, NMR spectroscopy, X-ray diffraction study.

Received: 14 March 2018/ Revised final: 02 May 2018/ Accepted: 02 May 2018

Introduction

The interest in the vanadium coordination chemistry stems from the catalytic activity of its compounds and their role in biological systems, as well as their use as therapeutic agents. Vanadium based catalysis is based mainly on the use of oxidovanadium complexes in high-oxidation states for various organic transformations [1-2]. Vanadium coordination compounds are recognized as promising drugs against diabetes of type I and type II, cancer and parasitic diseases [3-4]. Semicarbazones and thiosemicarbazones are well known due to their biological activities, which are considered related to their ability to form chelates with metals [5-7]. Synthesis and characterization of vanadium complexes with the derivatives based on these ligands is interesting from the view point of creation of more effective and selective therapeutic agents.

A detailed physicochemical characterization of vanadium complexes with salicylaldehyde semicarbazone derivatives, involving *in vitro* biological evaluation as potential insulin-mimetic and anti-tumour agents, of a series of novel (semicarbazone)VO₂⁺ complexes with the general formula *cis*-V^{VO}₂L have been reported [8-10]. In these complexes, the vanadium atom is in a distorted square-

pyramidal coordination, with semicarbazones acting as tridentate ligands. An interesting derivative of salicylaldehyde semicarbazone can be synthesized using related 3-methoxy-salicylaldehyde (*o*-vanillin). A new series of mixed-ligand oxidovanadium(IV) complexes, [V^{IV}O(L)(NN)], where L is bideprotonated *o*-vanillin semicarbazone (Figure 1), and NN is 1,10-phenanthroline derivatives, were recently reported [11,12]. The complexes showed higher *in vitro* anti-trypanosomal activities than the reference drug Nifurtimox and cytotoxicity on human promyelocytic leukemia HL-60 cells with IC₅₀ values of the same order of magnitude as cisplatin.

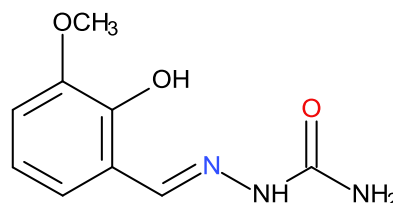


Figure 1. The *o*-vanillin semicarbazone ligand (H₂L).

In continuation of our research on vanadium coordination compounds with *o*-vanillin semicarbazone ligands, we present

here the synthesis and X-ray structure characterization of novel coordination complexes of oxidovanadium(V) $[\text{VO}(\text{HL})(\text{EtO})(\text{EtOH})_{0.6}(\text{H}_2\text{O})_{0.4}][\text{VO}(\text{HL})(\text{SO}_4)(\text{EtO})\cdot 0.4\text{EtOH}$ (**1**) and dioxidovanadium(V) $[\text{VO}_2(\text{HL})]\cdot 2\text{H}_2\text{O}$ (**2**), where H_2L is the *o*-vanillin semicarbazone ligand. NMR spectral studies of the complexes under discussion confirmed their structures in $\text{DMSO-}d_6$ solutions.

Experimental

Synthesis

All reagents and solvents were obtained from commercial sources and used without further purification.

The ligand, H_2L , was obtained by the reaction of *o*-vanillin with semicarbazide hydrochloride in the molar ratio 1:1 in warm EtOH solutions [13].

$[\text{VO}(\text{HL})(\text{EtO})(\text{EtOH})_{0.6}(\text{H}_2\text{O})_{0.4}][\text{VO}(\text{HL})(\text{SO}_4)]\cdot 0.4\text{EtOH}$ (**1**)

A mixture of $\text{VO}\text{SO}_4\cdot 2\text{H}_2\text{O}$ (0.20 g, 1 mmol) and *o*-vanillin semicarbazone (0.10 g, 0.5 mmol) in ethanol (20 mL) was heated on a water bath for 1 h. The clear brown solution was cooled, filtered and placed in a parafilm sealed vial. After two weeks brown needles, suitable for X-rays diffraction study, were filtered off, washed with ethanol, and dried in air. Yield: 30%. ^1H NMR (298K): δ 0.89 (t, $J= 6.9$, $-\text{CH}_2\text{CH}_3$), 0.90 (t, $J= 6.9$, $-\text{CH}_2\text{CH}_3$), 1.06 (t, $J= 6.8$, HOCH_2CH_3 of external sphere), 1.52 (t, $J= 6.8$, $-\text{CH}_2\text{CH}_3$), 3.45 (q, $J= 6.8$, HOCH_2CH_3 and $-\text{CH}_2\text{CH}_3$), 3.74 (s, $-\text{OCH}_3$, overlapped with the dissolved in $\text{DMSO-}d_6$ H_2O), 3.80 (s, $-\text{OCH}_3$, overlapped with the dissolved in $\text{DMSO-}d_6$ H_2O), 3.85 (s, $-\text{OCH}_3$, overlapped with the dissolved in $\text{DMSO-}d_6$ H_2O), 6.79 (3H, br. s. Ar), 7.05 (3H, br. s. Ar), 7.10 (3H, br. s. Ar), 8.08 (br. s, $-\text{NH}_2$), 8.59 (3H, br. s, $-\text{CH}=\text{N}$), 12.68 (br. s, protons of semicarbazone resonance species).

$[\text{VO}_2(\text{HL})]\cdot 2\text{H}_2\text{O}$ (**2**)

A solution of 25% NH_4OH (aq) (10 mL) was added to a NH_4VO_3 (0.06g; 0.5 mmol) and *o*-vanillin semicarbazone (0.10 g, 0.5 mmol) suspension in methanol (10 mL). The mixture was heated on a water bath for 1 h to form a yellow solution. It was filtered and the filtrate was allowed to stand at room temperature for crystallization. After two days the microcrystalline precipitate containing orange single crystals of **2** was filtered off, washed with methanol, diethyl ether and dried in air. Yield: 40%. ^1H NMR (298K): δ 3.72 (3H, s, $-\text{OCH}_3$), 5.94 (1H, br. s, $-\text{NH}_2$), 6.63 (1H, t, $J= 7.8$, Ar), 6.83 (1H, dd, $J= 7.8$, 1.4, Ar), 6.93 (1H, dd,

$J= 7.8$, 1.4, Ar), 7.11 (br. s, proton of semicarbazone resonance species), 8.30 (1H, s, $-\text{CH}=\text{N}$). ^{13}C NMR (298 K): δ 55.7 ($-\text{OCH}_3$), 113.1, 116.2, 122.7 (Ar-CH), 121.5 (A-Cq), 144.6 (CH=N), 149.5 (Ar-C-OMe), 153.4 (Ar-C-O-V), 169.1 (N-C=O). ^{15}N NMR (298 K): δ 68 ($-\text{NH}_2$), 238 ($\text{V}\leftarrow\text{N-NH-C}=\text{O}$) and $\text{V}\leftarrow\text{N-N}=\text{C-OH}$, resonance species), 311 (CH=N).

Characterisation

Infrared spectra were recorded on a Perkin-Elmer FTIR spectrophotometer in $4000\text{--}650\text{ cm}^{-1}$ region.

NMR spectra were recorded on a Bruker AVANCE 400 spectrometer equipped with a 5 mm broadband reverse probe with field z gradient, operating at 400.13, 100.61 and 40.54 MHz for ^1H , ^{13}C and ^{15}N nuclei, respectively. $\text{DMSO-}d_6$ (isotopic enrichment 99.95%) was used as solvent, containing tetramethylsilane (TMS) as an internal standard. Chemical shifts (δ) are reported in parts per million (ppm) and are referenced to the residual non-deuterated solvent peak (2.50 ppm for ^1H and 39.50 ppm for ^{13}C). Coupling constants (J) are reported in Hertz. The 1D (^1H , ^{13}C , DEPT-135) and 2D homo- ($^1\text{H}/^1\text{H}$ COSY-45) and heteronuclear ($^1\text{H}/^{13}\text{C}$ HSQC and $^1\text{H}/^{13}\text{C}$ HMBC), ($^1\text{H}/^{15}\text{N}$ HMQC and $^1\text{H}/^{15}\text{N}$ HMBC) NMR experiments were performed through standard pulse sequences. The ^{15}N NMR chemical shifts are reported relative to liquid NH_3 [14].

X-ray structure determination

Diffraction measurements for **1** and **2** were carried out at room temperature on an Xcalibur E diffractometer equipped with CCD area detector and a graphite monochromator utilizing $\text{MoK}\alpha$ radiation. Final unit cell dimensions were obtained and refined on an entire data set. All calculations to solve and refine the structures were carried out using SHELXS97 and SHELXL2014 programs [15,16]. Hydrogen atoms attached to carbon atoms were placed geometrically in idealized positions and refined in a riding model. The positions of H-atoms of water and ethanol molecules in **1** and **2** were located on difference Fourier maps. Crystallographic data were deposited with the Cambridge Crystallographic Data Centre and allocated the deposition numbers CCDC 1825937 (**1**) and 1825938 (**2**). These data can be obtained free of charge from the Cambridge Crystallographic Data Centre *via* www.ccdc.cam.ac.uk/data_request/cif.

Results and discussion

Vanadium complex **1** was prepared *via* the reaction of $\text{VO}\text{SO}_4\cdot 2\text{H}_2\text{O}$ with H_2L in a 2:1 molar

ratio in ethanol. During the reaction, vanadium(IV) is oxidized to vanadium(V). The reaction of NH_4VO_3 with H_2L in the 1:1 ratio in a methanol/ NH_4OH mixture afforded complex **2** in moderate yield.

The IR spectrum of the ligand H_2L shows stretching bands attributed to $\text{C}=\text{O}$, $\text{CH}=\text{N}$, and $\text{C}-\text{OH}$ (phenolic) at 1670, 1578, and 1263 cm^{-1} , respectively, whereas a band at 3465 cm^{-1} is assigned to $\nu(\text{O}-\text{H})$ vibrations involving intermolecular hydrogen bonding. The disappearance of the band at 3465 cm^{-1} in the spectra of compounds **1** and **2** supports the involvement of phenolic oxygen in coordination through deprotonation [17]. The $\nu(\text{CH}=\text{N})$ band seen at 1578 cm^{-1} in the free ligand spectrum is shifted towards higher wavenumbers in the

spectra of the complexes due to the involvement of the azomethine nitrogen in coordination. The $\nu(\text{C}=\text{O})$ band is also shifted to the lower energy region in the IR spectra of both complexes (1654 and 1620 cm^{-1}) indicating the keto form of coordinated ligand. Complex **2** also shows strong bands at around 913 and 862 cm^{-1} , which are assigned to antisymmetric and symmetric $\nu(\text{O}=\text{V}=\text{O})$ vibrations of the *cis*- VO_2 group, (also referred as pervanadyl), respectively.

Crystal structures

The crystal structures of **1** and **2** were determined by X-ray crystallography. Crystallographic data and structure refinement details for compounds **1** and **2** are summarized in Table 1 and selected geometric parameters are given in Table 2.

Table 1

Crystallographic data and structure refinement details for compounds **1** and **2**.

Parameters	Value	
Compound	1	2
Empirical formula	$\text{C}_{24}\text{H}_{36.8}\text{N}_6\text{O}_{15.4}\text{S}_1\text{V}_2$	$\text{C}_9\text{H}_{14}\text{N}_3\text{O}_7\text{V}_1$
Formula weight	789.83	327.11
Temperature (K)	293(2)	293(2)
Wavelength (\AA)	0.71073	0.71073
Crystal system	Monoclinic	Orthorhombic
Space group	$P2_1/n$	$P2_12_12_1$
Z	4	4
<i>a</i> (\AA)	21.7537(17)	5.8870(3)
<i>b</i> (\AA)	6.9686(5)	13.7731(6)
<i>c</i> (\AA)	23.7764(14)	16.1010(13)
α (deg)	90	90
β (deg)	100.570(8)	90
γ (deg)	90	90
<i>V</i> (\AA^3)	3543.2(5)	1305.51(14)
<i>D_c</i> (g/cm^{-3})	1.480	1.665
μ (mm^{-1})	0.660	0.796
F (000)	1632	672
Crystal size (mm^3)	0.42 x 0.18 x 0.05	0.4 x 0.1 x 0.08
Reflections collected/unique	11281/6230 [R(int) = 0.0567]	3239/2154 [R(int) = 0.0259]
Reflections with [$I > 2\sigma(I)$]	3387	1891
Nr parameters	452	194
GOF on F^2	1.002	1.001
R_1, wR_2 [$I > 2\sigma(I)$]	0.0816, 0.1828	0.0467, 0.1135
R_1, wR_2 (all data)	0.1543, 0.2184	0.0553, 0.1193

The ionic compound **1** comprises complex cations $[\text{VO}(\text{HL})(\text{EtO})(\text{EtOH})]^+$ and $[\text{VO}(\text{HL})(\text{EtO})(\text{H}_2\text{O})]^+$, and complex anions $[\text{VO}(\text{HL})(\text{SO}_4)(\text{EtO})]^-$, and partial occupancy solvent ethanol molecules (Figures 2 and 3). The crystals of compound **2** are build up from the neutral molecular complexes $[\text{VO}_2(\text{HL})]$ and solvent water molecules. In both compounds **1** and **2** the monoanionic ligand HL^- in keto form coordinates to metal atom in a tridentate mode *via* ONO donor atoms set. The complex cations

$[\text{VO}(\text{HL})(\text{EtO})(\text{EtOH})]^+$ and $[\text{VO}(\text{HL})(\text{EtO})(\text{H}_2\text{O})]^+$ in the structure of **1** are similar (Figure 2), occupy the same place in the crystal, and differ only by $\text{C}_2\text{H}_5\text{OH}$ or H_2O molecule coordinated to vanadium atom in *trans*-position to the oxido ligand. The positions of all atoms except carbon and hydrogen atoms of these coordinated solvent molecules are in accordance with the structure within the resolution of data, and structure refinement shows that $\text{C}_2\text{H}_5\text{OH}$ and H_2O molecules occupy their positions with a

probability of 0.6 and 0.4, respectively. The vanadium atoms V(1) in the complex cation and V(2) in the complex anion (Figure 3) have a distorted octahedral NO₅ surrounding provided by semicarbazone ligand, oxido, ethoxide, and ethanol/water oxygen atoms or oxygen atom of SO₄²⁻ anion, respectively. The ethoxido ligand is *trans*-situated with respect to the N(1A) atom. The vanadium–oxygen bond lengths follow the order V–O(oxido) < V–O(ethoxido) < V–O(phenoxido) < V–O(keto) < V–O(ethanol) < V–O(SO₄) (Table 2), indicating a stronger binding of the ethoxido group compared

with those of phenoxido and keto oxygen atoms [18] and weak coordination binding of solvent molecules or SO₄²⁻ anion in *trans*-position to oxido ligand. The weak coordination binding of SO₄²⁻ anion is also confirmed by S–O bonds length. The S–O(5B)=1.455(5) Å for the oxygen atom coordinated to the metal atom is shorter than S–O bonds 1.471(4) to 1.489 (5) Å for oxygen atoms participating only in classical H-bonds. The N(1)–N(2), N(2)–C(8), and C(8)–O(2) bonds have a partial double-bond character, which suggests that there is an electron delocalization within the semicarbazide fragment.

Table 2

Selected bond distances (Å) and angles (°) in metal coordination cores in **1** and **2**.

Complex 1			
Bond	<i>d</i> , Å	Bond	<i>d</i> , Å
V(1)–O(1V)	1.576(5)	V(2)–O(2V)	1.581(5)
V(1)–N(1A)	2.149(5)	V(2)–N(1B)	2.160(6)
V(1)–O(1A)	2.017(4)	V(2)–O(1B)	2.008(4)
V(1)–O(2A)	1.833(4)	V(2)–O(2B)	1.856(5)
V(1)–O(4A)/O(1W)	2.266(5)	V(2)–O(4B)	1.765(5)
V(1)–O(5A)	1.742(5)	V(2)–O(5B)	2.293(4)
Angle	<i>ω</i> , deg	Angle	<i>ω</i> , deg
O(1V)–V(1)–N(1A)	92.5(2)	O(2V)–V(2)–N(1B)	93.4(2)
O(1V)–V(1)–O(1A)	95.5(2)	O(2V)–V(2)–O(1B)	94.5(2)
O(1V)–V(1)–O(2A)	100.0(2)	O(2V)–V(2)–O(2B)	99.5(3)
O(1V)–V(1)–O(4A)	172.6(2)	O(2V)–V(2)–O(4B)	101.2(3)
O(1V)–V(1)–O(5A)	102.9(2)	O(2V)–V(2)–O(5B)	174.3(2)
N(1A)–V(1)–O(1A)	74.1(2)	N(1B)–V(2)–O(1B)	74.1(2)
N(1A)–V(1)–O(2A)	82.8(2)	O(1B)–V(2)–N(2B)	83.4(2)
N(1A)–V(1)–O(4A)	80.7(2)	N(1B)–V(2)–O(4B)	161.5(2)
N(1A)–V(1)–O(5A)	160.1(2)	N(1B)–V(2)–O(5B)	80.8(2)
O(1A)–V(1)–O(2A)	152.6(2)	O(1B)–V(2)–O(2B)	154.1(2)
O(1A)–V(1)–O(4A)	79.9(2)	O(1B)–V(2)–O(4B)	93.5(2)
O(1A)–V(1)–O(5A)	91.8(2)	O(1B)–V(2)–O(5B)	83.5(2)
O(2A)–V(1)–O(4A)	82.1(2)	O(2B)–V(2)–O(4B)	105.0(2)
O(2A)–V(1)–O(5A)	106.3(2)	O(2B)–V(2)–O(5B)	80.4(2)
O(4A)–V(1)–O(5A)	83.2(2)	O(4B)–V(2)–O(5B)	84.3(2)
Complex 2			
Bond	<i>d</i> , Å	Bond	<i>d</i> , Å
V(1)–O(1)	1.876(3)	V(1)–O(5)	1.641(3)
V(1)–O(2)	1.981(3)	V(1)–N(1)	2.165(3)
V(1)–O(4)	1.621(3)		
Angle	<i>ω</i> , deg	Angle	<i>ω</i> , deg
O(1)–V(1)–O(2)	144.6(2)	O(2)–V(1)–O(5)	91.2(2)
O(1)–V(1)–O(4)	107.2(2)	O(2)–V(1)–N(1)	74.0(1)
O(1)–V(1)–O(5)	97.5(2)	O(4)–V(1)–O(5)	107.6(2)
O(1)–V(1)–N(1)	82.0(1)	O(4)–V(1)–N(1)	100.8(2)
O(2)–V(1)–O(4)	102.6(2)	O(5)–V(1)–N(1)	150.4(2)

The N–H···O hydrogen bonds dominate in the crystal packing of **1**, due to amine functionality, and a crucial role is played by the sulphate ion, which provides the majority of the hydrogen-bond acceptors for the semicarbazone NH and NH₂ donor groups of both complex cations and anions. Moreover, the complex cation

and anion are additionally linked by strong intermolecular O–H···O hydrogen bonds involving coordinated sulphate ion, and coordinated molecules of C₂H₅OH/H₂O. In the crystal, N–H···O and O–H···O hydrogen bonds unite components in **1** into 1D chains running along *b* crystallographic axis (Table 3, Figure 4).

The parallel packing of such chains creates in the structure hydrophobic pockets filled with solvent ethanol molecules of partial occupancy 0.4 and correlates with the partial occupancy of coordinated water/ethanol molecules in the complex cation. The pockets may adopt solvent

ethanol molecules only when water occupies the sixth coordination position of V(1) atoms. The coordinated ethanol molecule results in a smaller size pocket, unsuitable for inclusion of solvent ethanol molecule.

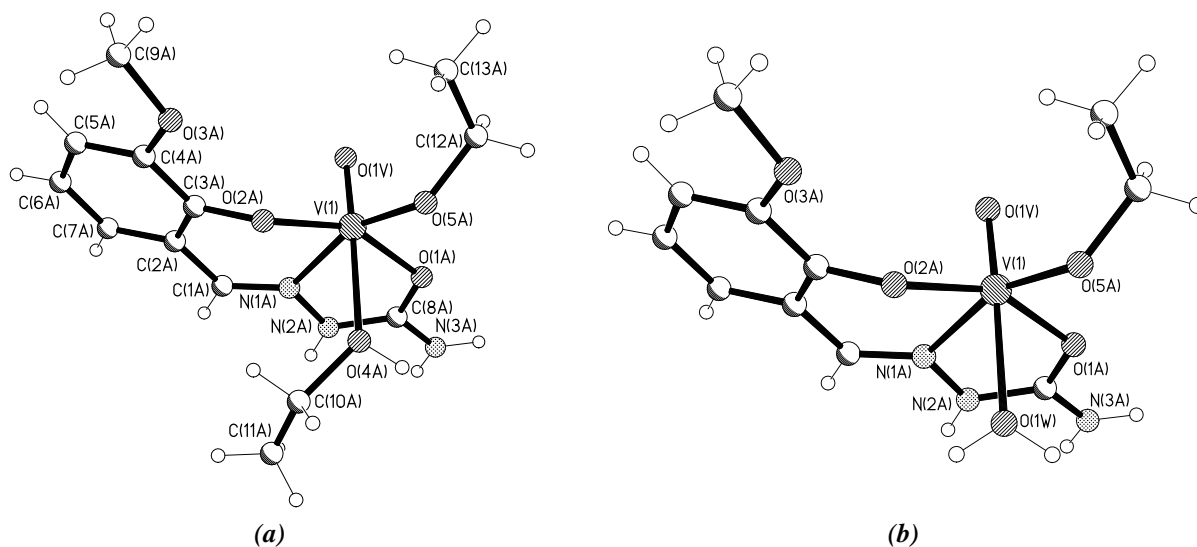


Figure 2. Structure of the complex cations of **1** showing coordination of ethanol (via O(4A), (a)) and water (via O(1W), (b)) molecules with the numbering scheme.

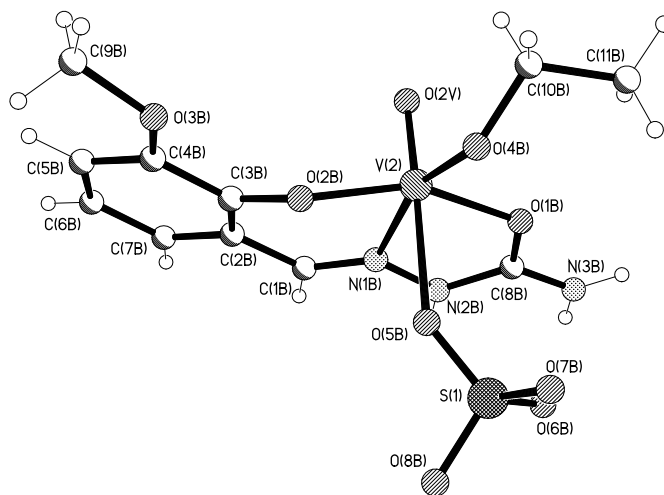


Figure 3. View of the molecular structure of the complex anion in compound **1** with atom numbering scheme.

The molecular structure of compound **2** with the composition $[\text{VO}_2(\text{HL})]\cdot 2\text{H}_2\text{O}$ is very similar to the recently reported coordination compound $[\text{VO}_2(\text{HL})]\cdot \text{C}_2\text{H}_5\text{OH}$ [19], but their crystal structures differ due to the difference in crystallization solvent molecules. The asymmetric unit of **2** contains a neutral complex with a pentavalent vanadium atom in a distorted square-pyramidal environment and two solvent water

molecules, one of which is disordered and occupies two positions with equal probability. The vanadium(V) atom in complex **2** adopts a distorted square-pyramidal environment (Figure 5). The *o*-vanillin semicarbazone ligand coordinates in ONO tridentate mode through the azomethine nitrogen atom, and carbonyl and deprotonated phenol oxygen atoms, and together with one oxido ligand form the base of a pyramid.

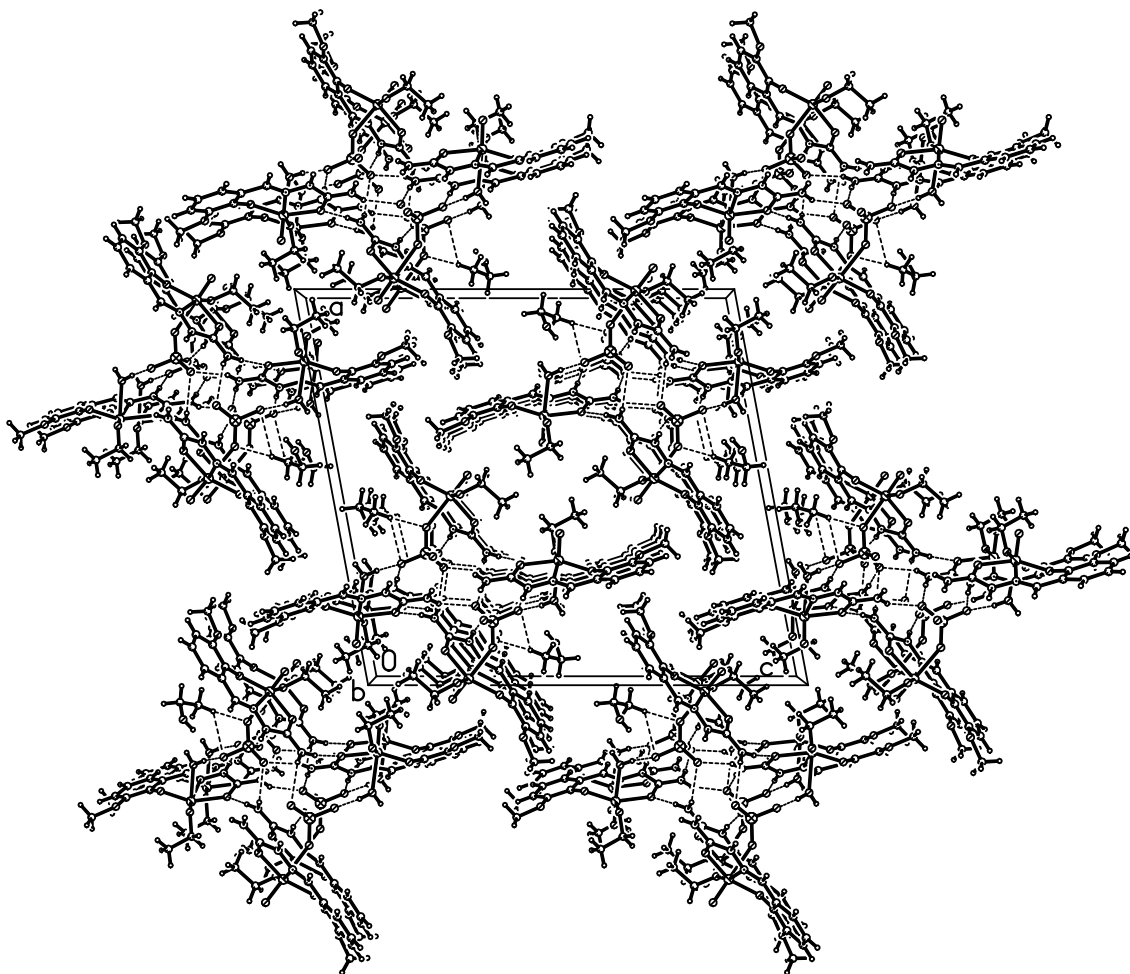


Figure 4. Chain and solvent molecules in the crystal structure of 1.

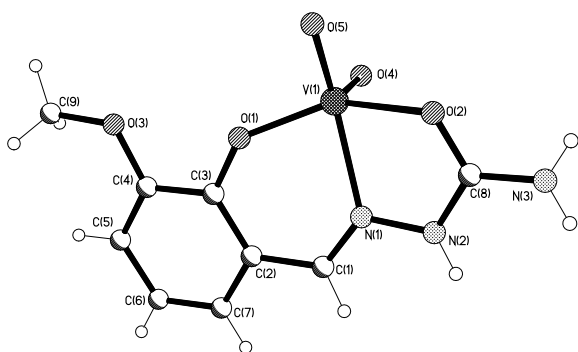


Figure 5. The molecular structure of complex 2 with atom numbering scheme.

Their vertex is occupied by another oxido ligand. The average V–O bond length and O–V–O angle (Table 2) are quite similar to those previously reported for the *cis*-VO₂ moiety in other complexes [8,9,19] (Figure 6). The vanadium atom square pyramidal coordination polyhedron geometry is confirmed by the general descriptor $\tau = (\beta - \alpha)/60 = 0.097$, where α and β are the two

largest angles at the metal center for five-coordinated complexes. For a perfect square-pyramidal geometry τ equals to zero, and it becomes unity for the perfect trigonal-bipyramidal geometry [20].

In the crystal of 2 the complexes are linked in chains running along *a* crystallographic axis by intermolecular N(3)–H···O(4) hydrogen bonds, involving the terminal NH groups of the semicarbazone ligand and the apical oxido ligand of neighbouring complexes. These parallel chains are united in a layer parallel to (*ab*) crystallographic plane through hydrogen bonds involving water molecules O1W: N(2)–H···O(1W) and O(1W)–H···O(5) (Table 3, Figure 6). The layers are H-bonded through disordered solvate water molecules O2W/O3W in a 3D network (Table 3). The structure is also stabilized by weak hydrogen bonds C(1)–H···O(4)/O5 ($-x+2, y+1/2, -z+1/2$) with (C(1)···O(4) 3.331 Å, H···O(4) 2.53 Å, $\angle(\text{CHO})$ 144°; C(1)···O(5) 3.372 Å, H···O(5) 2.55 Å, $\angle(\text{CHO})$ 147°) geometric parameters.

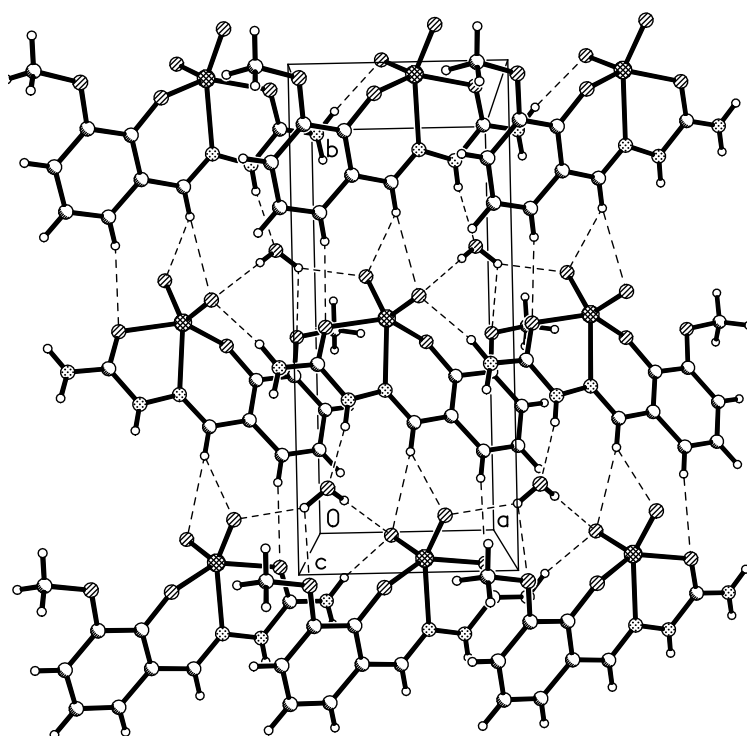


Figure 6. The hydrogen bonded layer in the structure of 2.

Table 3

Hydrogen bond distances (Å) and angles (°) in 1 and 2.				
<i>D-H...A</i>	<i>d(H...A)</i>	<i>d(D...A)</i>	$\angle(DHA)$	<i>Symmetry transformations for acceptor</i>
Complex 1				
N(2A)-H(1)···O(8B)	1.87	2.719(7)	170	<i>x, y+1, z</i>
N(3A)-H(1)···O(6B)	2.06	2.842(7)	150	$-x+1/2, y+1/2, -z+5/2$
N(3A)-H(2)···O(6B)	1.92	2.776(7)	173	<i>x, y+1, z</i>
O(4A)-H(1)···O(8B)	1.83	2.705(6)	171	<i>x, y, z</i>
O(1W)-H(1)···O(8B)	1.84	2.705(6)	167	<i>x, y, z</i>
N(2B)-H(1)···O(7B)	1.82	2.671(7)	170	<i>x, y-1, z</i>
N(3B)-H(1)···O(6B)	2.35	3.037(7)	137	$-x+1/2, y-1/2, -z+5/2$
N(3B)-H(2)···O(1A)	2.14	2.973(7)	163	$-x+1/2, y-1/2, -z+5/2$
Complex 2				
N(2)-H(1)···O(1W)	1.96	2.813(5)	171	$-x+2, y+1/2, -z+1/2$
N(3)-H(1)···O(4)	2.31	3.021(5)	140	<i>x+1, y, z</i>
N(3)-H(2)···O(3W)	2.08	2.92(3)	163	$-x+2, y+1/2, -z+1/2$
N(3)-H(2)···O(2W)	2.17	2.93(3)	148	$-x+2, y+1/2, -z+1/2$
O(1W)-H(2)···O(5)	2.12	2.806(5)	138	<i>x-1, y, z</i>
O(2W)-H(1)···O(1W)	2.33	3.01(4)	140	$x-1/2, -y+1/2, -z$
O(2W)-H(2)···O(5)	2.15	2.83(3)	139	<i>x-1, y, z</i>

NMR characterisation

The NMR data for the oxido- and dioxidovanadium(V) coordination compounds **1** and **2** are consistent with the determined molecular structures. In the case of complex **1**, the ^1H NMR data are in line with the known reports regarding its congeners [13,19]. It should be mentioned, that for compound **1** the NMR investigation was hindered by its low solubility and by its dissociation in the $\text{DMSO}-d_6$ solution.

Due to the low sensitivity of ^{13}C and ^{15}N nuclei, reliable NMR spectral data for these nuclei in compound **1** were not obtained. Nevertheless, HETCOR experiments allowed the assignment of all ^1H signals in its spectrum. In the ^1H NMR spectrum of complex **1** most of the signals are broadened (Figure 7(a)), in contrast to the reported data for analogous diamagnetic compounds [13,19]. Both broadening of the signals characteristic for aromatic protons and (δ 6.79,

7.05 and 7.10 ppm) and lack of their typical spin-spin splitting patterns can be explained by resonance overlapping, which is favourable for the presence of structurally close dissociated species (two cations and one anion) of complex **1**. Typical broad singlets in the spectrum can be assigned to the hydrogen atoms involved in proton exchange with residual molecules of water (δ 8.08 ppm, amine hydrogen atoms; 12.68 ppm, semicarbazone proton of the resonance species). Assignment of the broad signal at 12.68 ppm to a proton belonging to the resonance forms of semicarbazone is consistent with the XRD analysis, which ascertained bond delocalization in the discussed fragment. It should be mentioned that integration of the signals in ^1H spectrum is approximate, because of the afore-mentioned resonance overlapping, proton exchange phenomena, as well as overlapping with the signal of residual water in DMSO- d_6 (e.g. sharp singlets of methoxy groups at δ 3.74, 3.80 and 3.85 ppm are overlapped by water signal at δ 3.57 ppm, (Figure 7 (b)). It is noteworthy that the values of chemical shifts for the methoxy groups (δ 3.74, 3.80 and 3.85 ppm) corroborate the data of X-ray analysis on their non-participation in coordination to metal center, since $\Delta\delta$ is negligible ($\Delta\delta = \delta_{\text{complex}} - \delta_{\text{ligand}}$; for δ_{ligand} the following values are available: 3.80 ppm and 3.81 ppm [19]). In the ions of complex **1**, the azomethine anisotropic effect causes an upfield shift (by *cca.* 0.29 ppm) for the aromatic protons at δ 7.10 ppm (*cca.* δ 7.39 ppm in ligand), as recently was mentioned for vanadium(V) complexes of similar structure [13,19]. At the same time, a deshielding effect of the metal was also found upon protons of amine group (δ 6.42 ppm in ligand \rightarrow 8.08 ppm in ions of complex **1**), the azomethine moiety (δ 8.20 ppm in ligand \rightarrow 8.59 ppm in ions of complex **1**) and the semicarbazone proton of the resonance species (δ 10.22 ppm in ligand \rightarrow 12.68 ppm in ions of complex **1**). Ethyl groups of different species present in complex **1** could be distinguished with the help of ^1H - ^1H COSY-45 experiment. Thus, the COSY spectrum displays strong cross-peak between intensive triplet at δ 1.06 ppm and quartet at δ 3.45 ppm that has been assigned to the ethanol from the external sphere of complex and, most probably, coordinated ethanol of complex cation of **1**. The small triplets at δ 0.89, 0.90 and 1.52 ppm giving vicinal proton-proton coupling with the same quartet at δ 3.45 ppm were attributed to the ethoxy groups covalently bound to the metal.

^1H , ^{13}C and ^{15}N NMR spectral studies of complex **2** confirmed its structure in the

DMSO- d_6 solution. ^1H , ^{13}C and ^{15}N NMR data for complex **2** are presented in Figures S1-S7. Comparative investigation of ^{15}N nuclei for the complex under discussion and its ligand in the uncoordinated form has been accomplished for the first time. It allowed a better understanding of the phenomena regarding the π -delocalization along the semicarbazone moiety and contributed to avoiding of any misinterpretation for ^1H nuclei belonging to the same fragment, as well.

The chemical shift for magnetically equivalent protons of the methoxy group in complex **2** is found in its ^1H NMR spectrum at δ 3.72 ppm, supporting its non-participation in coordination to the metal, as previously mentioned for complex **1**. An upfield shift for the aromatic proton at δ 6.93 ppm is observed, caused by the azomethine anisotropic effect. At the same time, the proton of azomethine moiety resonated at δ 8.30 ppm. The broad singlet at δ 12.48 ppm characterizing the amide proton is absent in the ^1H spectrum of compound **2**, instead, the very broad singlet at δ 7.11 ppm is present, which was assigned to the semicarbazone proton of the resonance species. Extended π -delocalization along the semicarbazone fragment in DMSO- d_6 solution of complex **2** has been demonstrated by $^1\text{H}/^{15}\text{N}$ HMQC and $^1\text{H}/^{15}\text{N}$ HMBC NMR experiments that furnished a conclusive evidence for the co-existence of the resonance forms of complex **2** in DMSO- d_6 solution. Thus, in the $^1\text{H}/^{15}\text{N}$ HMQC spectrum of *o*-vanillin semicarbazone cross-peaks at δ 6.47/77 ppm and 10.25/155 ppm characterized the hydrogen and nitrogen nuclei of amine and amide fragments, respectively (Figure S8). In complex **2** both nuclei of amine function show an upfield shift (δ 5.94/69 ppm), whilst an amide proton was not detected. According to the data from $^1\text{H}/^{15}\text{N}$ HMBC experiments, the azomethine proton in the uncoordinated ligand at δ 8.20 ppm showed long-range correlation with the imine nitrogen at δ 315 ppm (stronger) and amide nitrogen δ 155 ppm (weaker) (Figure S9). In the $^1\text{H}/^{15}\text{N}$ HMBC spectrum of complex **2**, two cross-peaks are present for the imine proton at δ 8.30 ppm: with nitrogen nuclei at δ 238 ppm and δ 311 ppm. Both experimental values of chemical shifts for these particular semicarbazone nitrogen nuclei exclude the involvement of pure keto- form of the ligand in the coordination to metal, being an obvious indication on the afore-mentioned extended π -delocalization along the semicarbazone chain also occurring in DMSO- d_6 solution, as afore-discussed for the crystal structure of this complex.

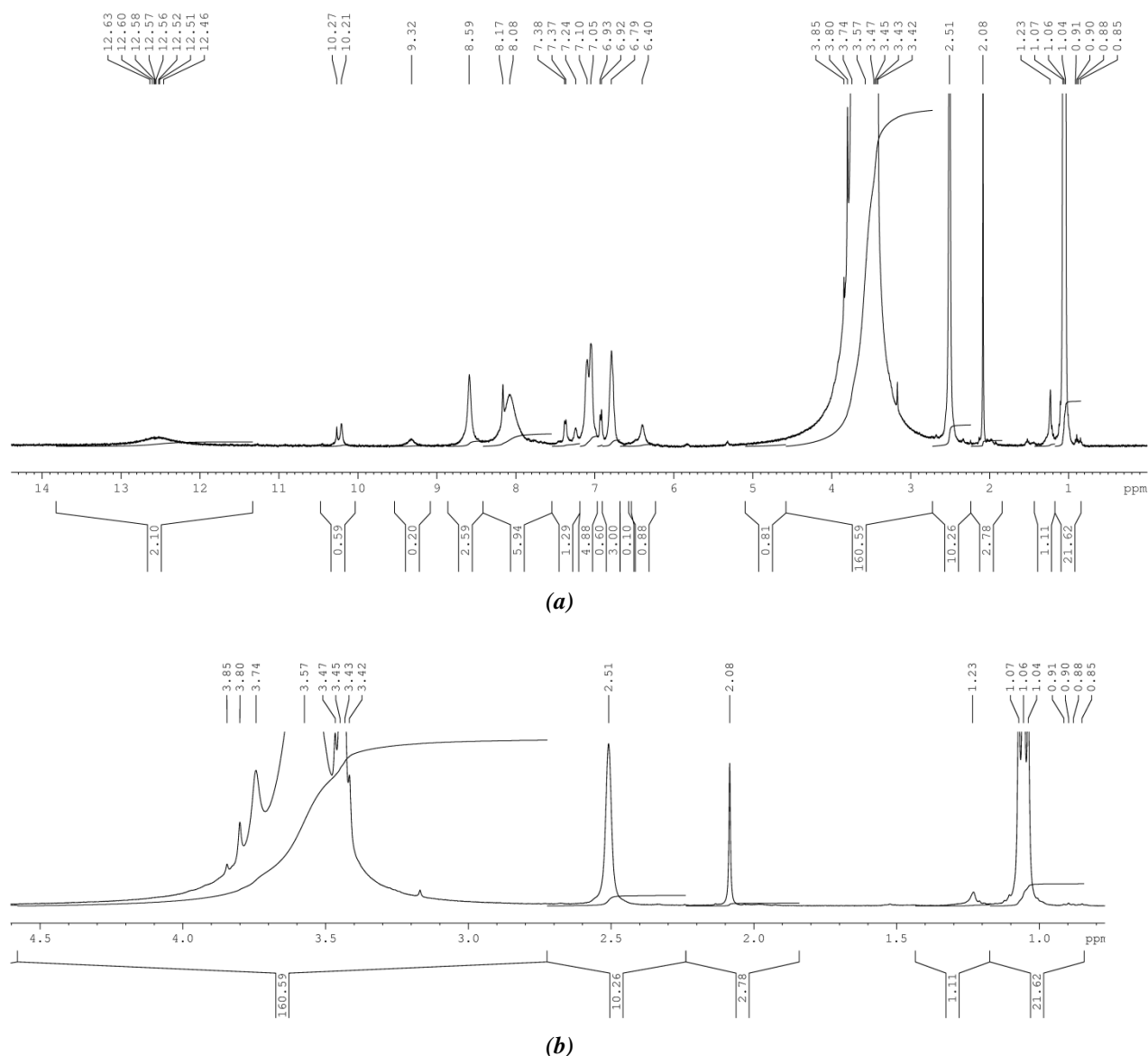


Figure 7. ¹H NMR spectrum of complex 1: (a) full spectrum, (b) region of 0.5-4.5 ppm of the spectrum.

Conclusions

In summary, we have synthesized and characterized by single-crystal X-ray crystallography two mononuclear vanadium(V) complexes comprising VO³⁺ and VO₂⁺ cores. The coordination polyhedra are an O₅N distorted octahedron in the mono-oxidovanadium complex **1** and a O₄N square-pyramid in the dioxidovanadium compound **2**. The formed solid state mononuclear structures are preserved in solution, as confirmed by multinuclear NMR experiments. For the first time, a comparative investigation of ¹⁵N nuclei for *o*-vanillin semicarbazone and complex **2** has been reported. The data obtained from ¹H/¹⁵N HETCOR experiments in DMSO-*d*₆ solution corroborate the results of X-ray studies on the existence of extended π -delocalization along the

semicarbazone fragment. This observation demonstrates the co-existence of the resonance forms of complex **2** in DMSO-*d*₆ solution.

Supplementary information

Supplementary data are available free of charge at <http://cjm.asm.md> as PDF file.

References

- da Silva, J.A.L.; Frausto da Silva, J.J.R.; Pombeiro, A.J.L. Oxovanadium complexes in catalytic oxidations. *Coordination Chemistry Reviews*, 2011, 255(19-20), pp. 2232-2248. DOI: <https://doi.org/10.1016/j.ccr.2011.05.009>
- Sutradhar, M.; Martins, L.M.D.R.S.; Guedes da Silva, M.F.C.; Pombeiro, A.J.L. Vanadium complexes: recent progress in oxidation catalysis. *Coordination Chemistry Reviews*, 2015, 301-302, pp. 200-239.

- DOI: <https://doi.org/10.1016/j.ccr.2015.01.020>
- Tracey, A.S.; Willsky, G.R.; Takeuchi, E.S. Vanadium Chemistry, Biochemistry, Pharmacology and Practical Applications. CRC Press: Boca Raton, London, New York, 2007, 250 p. <https://www.crcpress.com/>
 - Kustin, K.; Pessoa, J.C.; Crans, D.C. Eds. Vanadium: The Versatile Metal, ACS Symposium Series, 974, American Chemical Society: Washington DC, 2007, 352 p. DOI: [10.1021/bk-2007-0974.fw001](https://doi.org/10.1021/bk-2007-0974.fw001)
 - Padhye, S.; Kauffman, G.B. Transition metal complexes of semicarbazones and thiosemicarbazones. Coordination Chemistry Reviews, 1985, 63, pp. 127-160. DOI: [https://doi.org/10.1016/0010-8545\(85\)80022-9](https://doi.org/10.1016/0010-8545(85)80022-9)
 - Casas, J.S.; Garcia-Tesende, M.S.; Sordo, J. Main group metal complexes of semicarbazones and thiosemicarbazones. A structural review. Coordination Chemistry Reviews, 2000, 209(1), pp. 197-261. DOI: [https://doi.org/10.1016/S0010-8545\(00\)00363-5](https://doi.org/10.1016/S0010-8545(00)00363-5)
 - Lobana, T.S.; Sharma, R.; Bawa, G.; Khanna, S. Bonding and structure trends of thiosemicarbazone derivatives of metals – An overview. Coordination Chemistry Reviews, 2009, 253(7-8), pp. 977-1055. DOI: <https://doi.org/10.1016/j.ccr.2008.07.004>
 - Noblia, P.; Baran, E.J.; Otero, L.; Draper, P.; Cerecetto, H.; Gonzalez, M.; Piro, O.E.; Castellano, E.E.; Inohara, T.; Adachi, Y.; Sakurai, H.; Gambino, D. New vanadium(V) complexes with salicylaldehyde semicarbazone derivatives: synthesis, characterization, and *in vitro* insulin-mimetic activity - crystal structure of [V^VO₂(salicylaldehyde semicarbazone)]. European Journal of Inorganic Chemistry, 2004, 2, pp. 322-328. DOI: <https://doi.org/10.1002/ejic.200300421>
 - Noblia, P.; Vieites, M.; Parajon-Costa, B.S.; Baran, E.J.; Cerecetto, H.; Draper, P.; Gonzalez, M.; Piro, O.E.; Castellano, E.E.; Azqueta, A.; Lopez de Cerain, A.; Monge-Vega, A.; Gambino, D. Vanadium(V) complexes with salicylaldehyde semicarbazone derivatives bearing *in vitro* anti-tumor activity toward kidney tumor cells (TK-10): crystal structure of [V^VO₂(5-bromosalicylaldehyde semicarbazone)]. Journal of Inorganic Biochemistry, 2005, 99(2), pp. 443-451. DOI: <https://doi.org/10.1016/j.jinorgbio.2004.10.019>
 - Rivadeneira, J.; Barrio, D.A.; Arrambide, G.; Gambino, D.; Bruzzone, L.; Etcheverry, S.B. Biological effects of a complex of vanadium(V) with salicylaldehyde semicarbazone in osteoblasts in culture: Mechanism of action. Journal of Inorganic Biochemistry, 2009, 103(4), pp. 633-642. DOI: <https://doi.org/10.1016/j.jinorgbio.2008.11.009>
 - Benítez, J.; Becco, L.; Correia, I.; Leal, S.M.; Guiset, H.; Pessoa, J.C.; Lorenzo, J.; Tanco, S.; Escobar, P.; Moreno, V.; Garat, B.; Gambino, D. Vanadium polypyridyl compounds as potential antiparasitic and antitumoral agents: New achievements. Journal of Inorganic Biochemistry, 2011, 105(2), pp. 303-312. DOI: <https://doi.org/10.1016/j.jinorgbio.2010.11.001>
 - Fernández, M.; Varela, J.; Correia, I.; Birriel, E.; Castiglioni, J.; Moreno, V.; Pessoa, J.C.; Cerecetto, H.; González, M.; Gambino, D. A new series of heteroleptic oxidovanadium(IV) compounds with phenanthroline-derived co-ligands: selective *Trypanosoma cruzi* growth inhibitors. Dalton Transactions, 2013, 42(33), pp. 11900-11911. DOI: <https://doi.org/10.1039/C3DT50512J>
 - Binil, P.S.; Anoop, M.R.; Suma, S.; Sudarsanakumar, M.R. Growth, spectral, and thermal characterization of 2-hydroxy-3-methoxybenzaldehyde semicarbazone. Journal of Thermal Analysis and Calorimetry, 2013, 112(2), pp. 913-919. DOI: <https://doi.org/10.1007/s10973-012-2601-2>
 - Mason, J. Nitrogen NMR. Encyclopedia of Magnetic Resonance, John Wiley & Sons: New Jersey, 2007, pp. 1-30. DOI: <https://doi.org/10.1002/9780470034590.emrstm0343>
 - Sheldrick, G.M. A short history of SHELX. Acta Crystallographica Section A, 2008, A64, pp. 112-122. DOI: <https://doi.org/10.1107/S0108767307043930>
 - Sheldrick, G.M. Crystal structure refinement with SHELXL. Acta Crystallographica Section C, 2015, C71, pp. 3-8. DOI: <https://doi.org/10.1107/S2053229614024218>
 - Monfared, H.H.; Alavi, S.; Bikas, R.; Vahedpour, M.; Mayer, P. Vanadiumoxo–aroylhydrazone complexes: Synthesis, structure and DFT calculations. Polyhedron, 2010, 29(18), pp. 3355-3362. DOI: <https://doi.org/10.1016/j.poly.2010.09.029>
 - Sutradhar, M.; Pombeiro, A.J.L. Coordination chemistry of non-oxido, oxido and dioxidovanadium(IV/V) complexes with azine fragment ligands. Coordination Chemistry Reviews, 2014, 265, pp. 89-124. DOI: <https://doi.org/10.1016/j.ccr.2014.01.007>
 - Fernández, M.; Becco, L.; Correia, I.; Benítez, J.; Piro, O.E.; Echeverria, G.A.; Medeiros, A.; Comini, M.; Lavaggi, M.L.; González, M.; Cerecetto, H.; Moreno, V.; Pessoa, J.C.; Garat, B.; Gambino, D. Oxidovanadium(IV) and dioxidovanadium(V) complexes of tridentate salicylaldehyde semicarbazones: Searching for prospective antitrypanosomal agents. Journal of Inorganic Biochemistry, 2013, 127, pp. 150-160. DOI: <https://doi.org/10.1016/j.jinorgbio.2013.02.010>
 - Addison, A.W.; Rao, T.N.; Reedijk, J.; van Rijn, J.; Verschoor, G.C. Synthesis, structure, and spectroscopic properties of copper(II) compounds containing nitrogen-sulphur donor ligands; the crystal and molecular structure of aqua[1,7-bis(N-methylbenzimidazol-2'-yl)-2,6-dithiaheptane] copper(II) perchlorate. Journal of the Chemical Society, Dalton Transactions, 1984, 0(7), pp. 1349-1356. DOI: <https://doi.org/10.1039/DT9840001349>